

## Supporting Information

# Three dimensional hierarchically porous crystalline MnO<sub>2</sub> structure design for high rate performance lithium-ion battery anode

Shikun Liu,<sup>a</sup> Xusong Liu,<sup>a</sup> Jiupeng Zhao,<sup>\*a</sup> Zhongqiu Tong,<sup>b</sup> Jing Wang,<sup>a</sup> Xiaoxuan Ma,<sup>a</sup> Caixia Chi,<sup>a</sup> Dapeng Su,<sup>a</sup> Xiaoxu Liu,<sup>\*ac</sup> Yao Li,<sup>\*b</sup>

*a MIIT Key Laboratory of Critical Materials Technology for New Energy Conversion and Storage, School of Chemistry and Chemical Engineering, Harbin Institute of Technology, Harbin 150001, PR China*

*b Center for Composite Materials Harbin Institute of Technology, Harbin 150001, PR China*

*c Heilongjiang University of Science and Technology, Harbin 150022, PR China*

*\*Corresponding authors. E-mail: jpzhao@hit.edu.cn; liu88062321@163.com;  
yaoli@hit.edu.cn*

## Electrodeposited Processes of Manganese Dioxide:

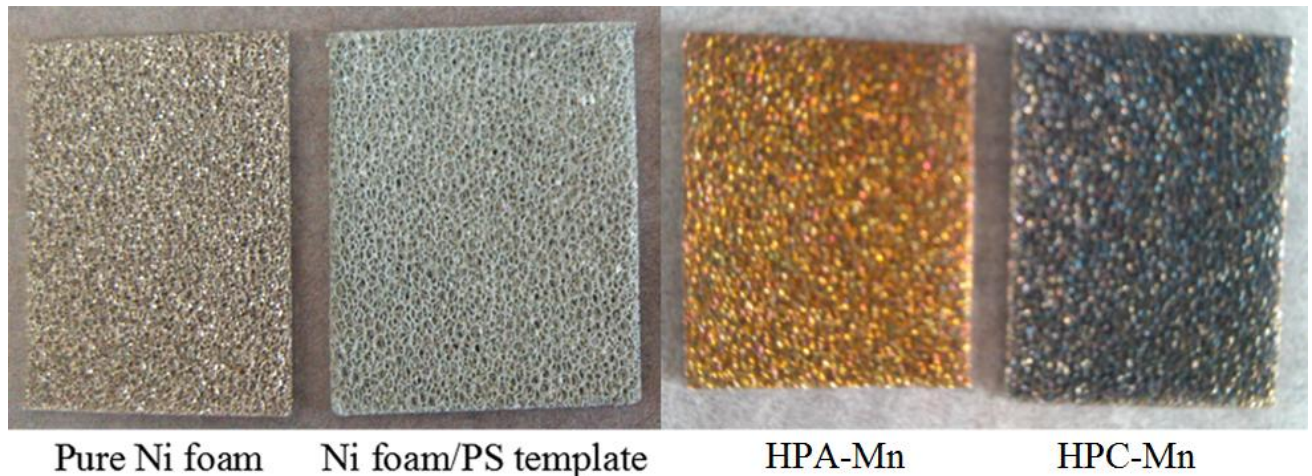


**Fig. S1** Optical image of Ni foam substrate, Ni foam/PS template, HPA-Mn and HPC-Mn samples

directly grown on Ni foam.

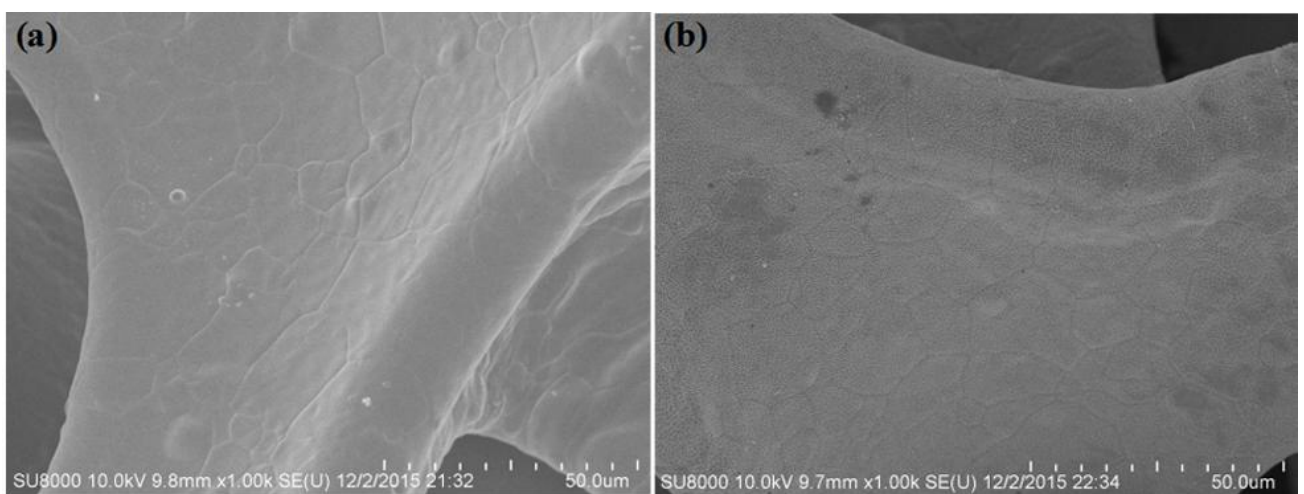


**Fig. S2** Low resolution SEM images of (a) pure Ni foam and (b) HPC-Mn sample.

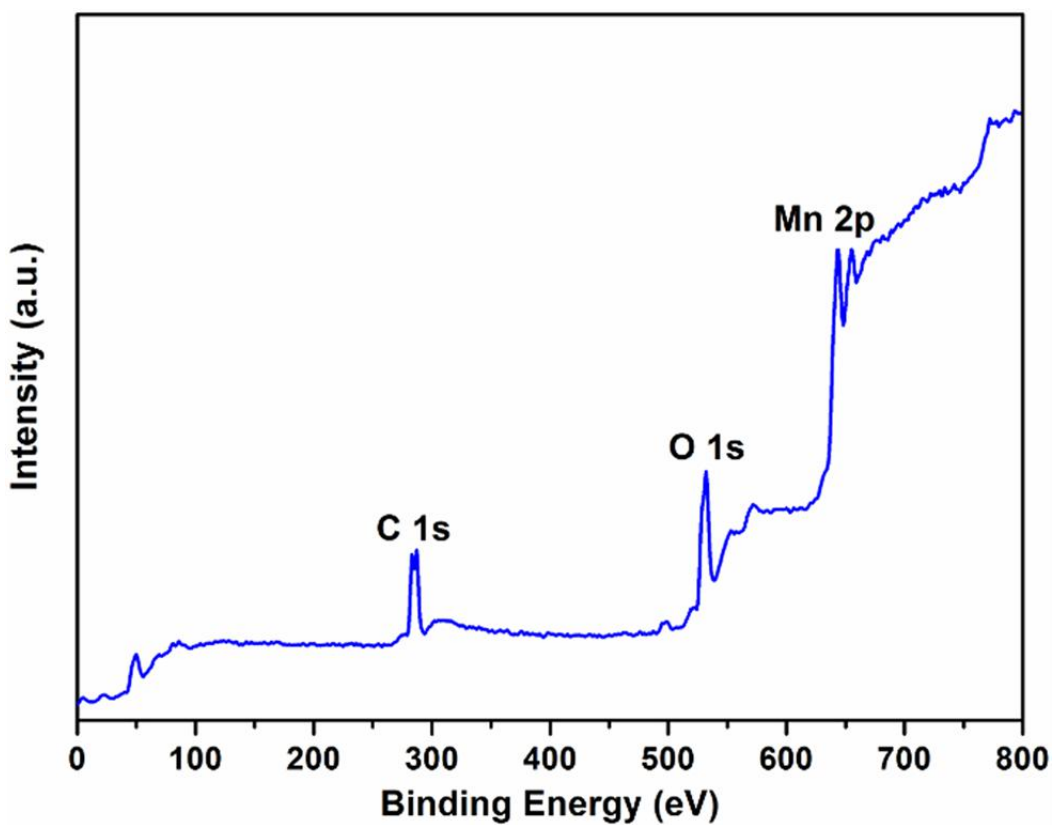


**Fig. S3** The wide scan XPS spectrum of HPC-Mn sample.

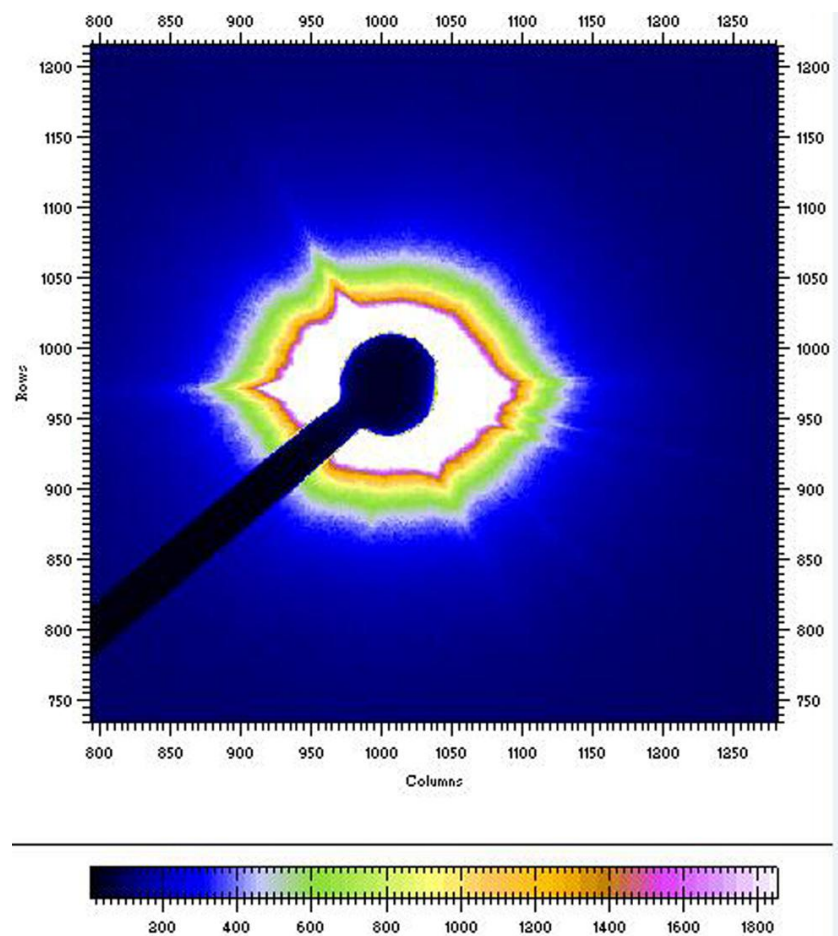


**Fig. S4** Two-dimensional SAXS patterns of HPA-Mn anode.

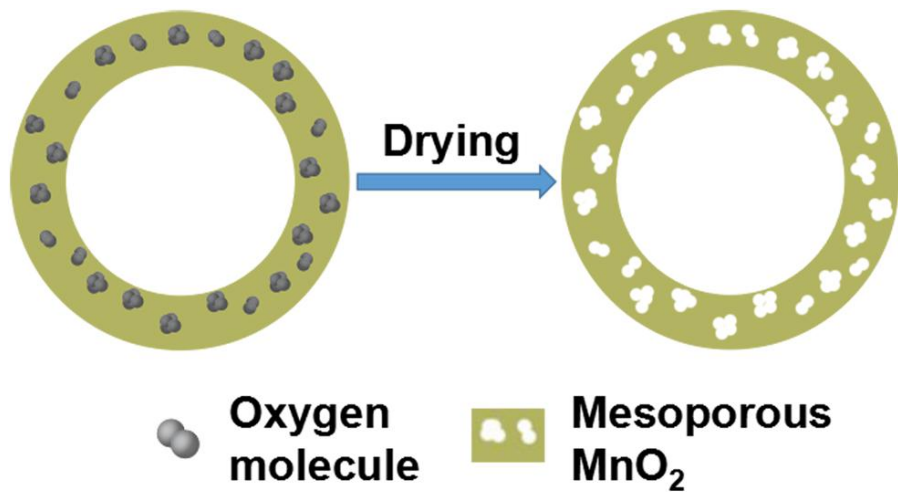


**Fig. S5** Schematic representation of the mesoporous formation assisted by oxygen.

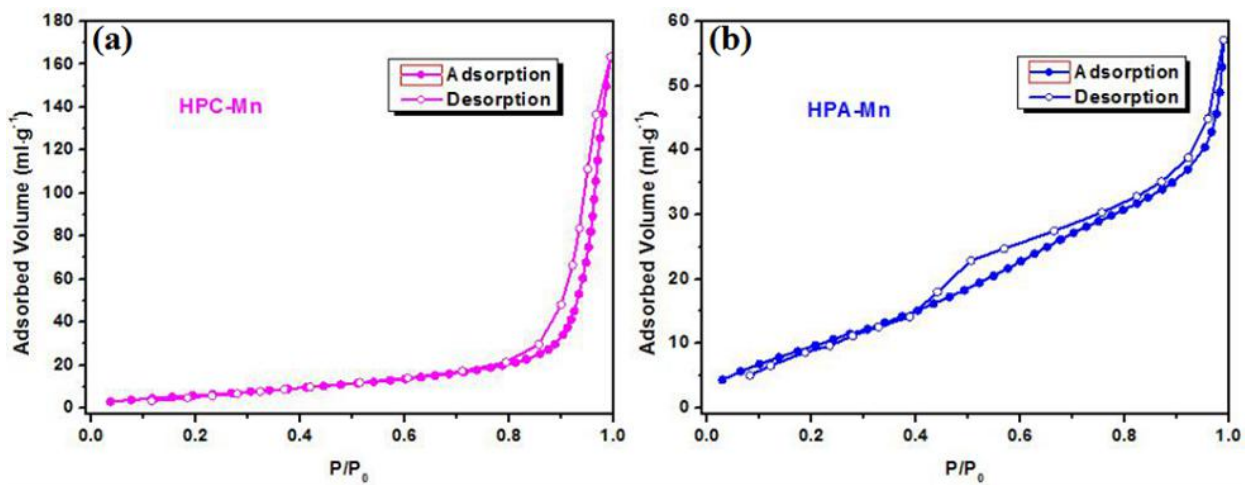


**Fig. S6** N<sub>2</sub> adsorption-desorption isotherms of (a) HPC-Mn anode and (b) HPA-Mn anode.

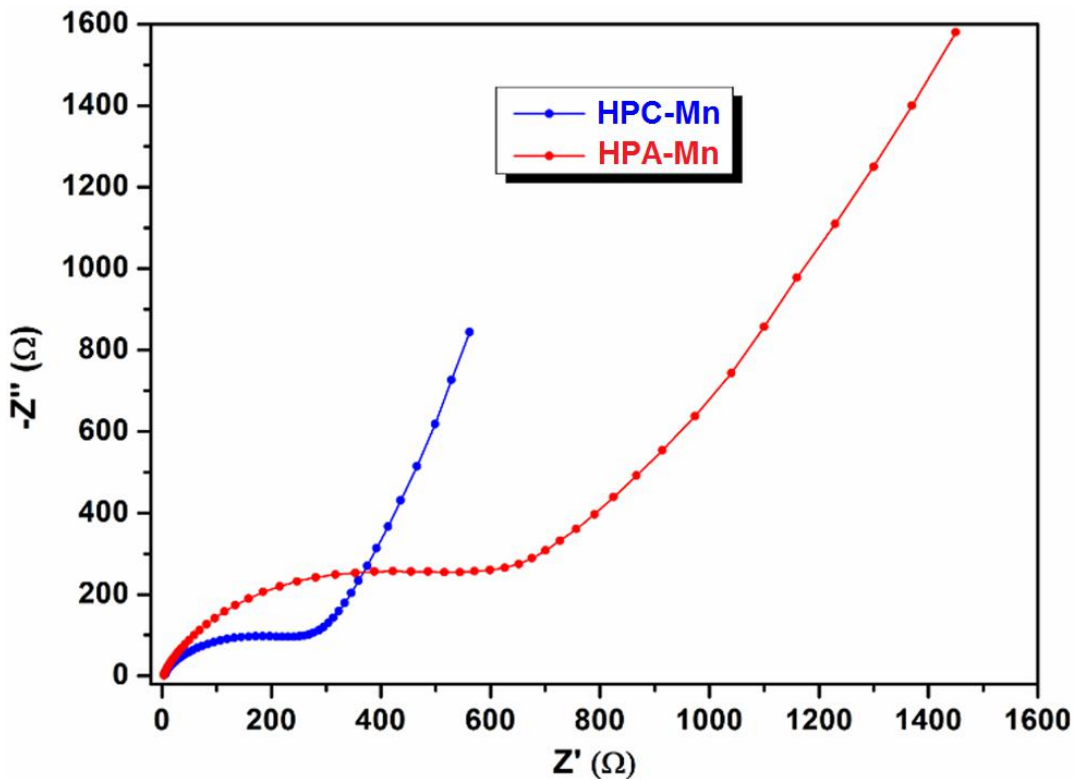


**Fig. S7** Nyquist plots of HPC-Mn and HPA-Mn anodes.

**Table S1** Rate performance comparison of the HPC-Mn and other reported MnO<sub>2</sub>-based anodes for LIBs.

MnO <sub>2</sub> Based Anodes	Low Current Density (A g <sup>-1</sup> ) Capacity (mAh g <sup>-1</sup> )	High Current Density (A g <sup>-1</sup> ) Capacity (mAh g <sup>-1</sup> )	Current Density Ratio	Capacity Retention (%)	Ref.
HPC-Mn	0.1 (973.8)	2.0 (798.8)	20	~82.0	Our Work
MnO <sub>2</sub> /3D porous graphene	0.1 (926.0)	1.6 (433.0)	16	~46.8	1
MnO <sub>2</sub> network-Ni/PVDF double shell/core fiber	0.05 (1079.0)	0.6 (544.7)	12	~50.5	2
MnO <sub>2</sub> @N-doped carbon nanotubes	0.05 (1146.0)	1.0 (620.7)	20	~54.2	3
Freestanding MnO <sub>2</sub> /Ni /PVDF coaxial fiber	0.05 (1178.4)	1.0 (415.0)	20	~35.2	4
MnO <sub>2</sub> on 3D N-doped graphene hybrid aerogels	0.1 (1003.0)	1.5 (636.0)	15	~63.4	5
MnO <sub>2</sub> nanoflakes on reduced graphene oxide nanosheets	0.1 (1430.0)	2.0 (1000.0)	20	~69.9	6
Nanoflaky MnO <sub>2</sub> on carbon microbeads	0.1 (700.0)	1.5 (230.0)	15	~32.9	7
Mesoporous MnO <sub>2</sub> nanosheet arrays	0.1 (-)	1.0 (-)	10	~50.0	8
Nanoflaky MnO <sub>2</sub> /carbon nanotube	0.2 (820.0)	2.0 (420.0)	10	~51.2	9

**Table S2** Cycling performance comparison of the HPC-Mn and other reported MnO<sub>2</sub>-based anodes for LIBs.

MnO <sub>2</sub> Based Anodes	Current Density (A g <sup>-1</sup> )	Cycling Number	Specific Capacity (mA h g <sup>-1</sup> ) After Cycling	Capacity Retention (%)	Ref.
HPC-Mn	0.4	200	778.0	~97.6	Our Work
MnO <sub>2</sub> /3D porous graphene	0.1	100	836.0	~84.6	1
MnO <sub>2</sub> network-Ni/PVDF double shell/core fiber	0.2	70	500.2	-	2
MnO <sub>2</sub> @N-doped carbon nanotubes	0.1	100	1415.0	>100	3
Freestanding MnO <sub>2</sub> /Ni /PVDF coaxial fiber	0.05	70	1031.2	-	4
MnO <sub>2</sub> on 3D N-doped graphene hybrid aerogels	0.4	200	909.0	>100	5
MnO <sub>2</sub> nanoflakes on reduced graphene oxide nanosheets	1.0	200	1000.0	~100	6
Nanoflaky MnO <sub>2</sub> on carbon microbeads	0.1	100	525.0	-	7
Mesoporous MnO <sub>2</sub> nanosheet arrays	1.0	200	900.0	>100	8
Nanoflaky MnO <sub>2</sub> /carbon nanotube	0.2	50	620.0	~77.0	9

**Note:** The specific capacities of some MnO<sub>2</sub> based anodes would increase with the increase of cycling number, so the capacity retention is >100%.

## References:

- Y. Y. Li, Q. W. Zhang, J. L. Zhu, X. L. Wei and P. K. Shen, *J. Mater. Chem. A*, 2014, **2**, 3163.
- Y. Zhang, Q. Xiao, G. Lei and Z. Li, *Phys. Chem. Chem. Phys.*, 2015, **17**, 18699.
- J. Yue, X. Gu, X. L. Jiang, L. Chen, N. N. Wang, J. Yang and X. J. Ma, *Electrochim. Acta*, 2015, **182**, 676.

- 4 Y. Zhang, Z. P. Luo, Q. Z. Xiao, T. L. Sun, G. T. Lei, Z. H. Li and X. J. Li, *J. Power Sources*, 2015, **297**, 442.
- 5 Z. Y. Sui, C. Wang, K. Shu, Q. S. Yang, Y. Ge, G. G. Wallace and B. H. Han, *J. Mater. Chem. A*, 2015, **3**, 10403.
- 6 Y. Cao, X. Lin, C. Zhang, C. Yang, Q. Zhang, W. Hu, M. Zheng and Q. Dong, *RSC Adv.*, 2014, **4**, 30150.
- 7 H. Wang, J. Liu, X. Wang, C. Wu, Q. Zhao, Y. Fu, X. Yang and H. Shu, *RSC Adv.*, 2014, **4**, 22241.
- 8 M. Kundu, C. C. A. Ng, D. Y. Petrovykh and L. F. Liu, *Chem. Commun.*, 2013, **49**, 8459.
- 9 H. Xia, M. O. Lai and L. Lu, *J. Mater. Chem.*, 2010, **20**, 6896.